The Madden Julian Oscillation in the ECMWF monthly forecasting system

Frédéric Vitart

ECMWF, Shinfield Park, Reading
RG2 9AX, United Kingdom
F.Vitart@ecmwf.int

ABSTRACT

A monthly forecasting system has been set up at ECMWF to fill the gap between the medium-range and the seasonal forecasting systems. It is based on 32-days coupled ocean-atmospheric integrations. This system has been run routinely since March 2002 every 2 weeks and 30 real-time forecasts have been used for the present study. The skill of the monthly forecasting system to predict the evolution of the Madden-Julian Oscillation (MJO) is investigated, through an EOF analysis of velocity potential at 200 hPa.

Results suggest that the model has some sill in predicting the propagation of the MJO up to about 20 days. However, the variance of the 200 hPa velocity potential tends to be reduced by a factor 2 after about only 10 days. This suggests that the model is likely to underestimate the impact of the MJO propagation on the large-scale circulation. A study of individual forecasts suggests that the model has difficulties to propagate the MJO from the Indian Ocean to the western Pacific.

1 Introduction

The monthly forecasting system fills the gap between the two currently operational forecasting systems at ECMWF: medium-range weather forecasting and seasonal forecasting. Therefore, the monthly forecasting system has been built as a combination of the medium-range EPS and the seasonal forecasting system. It contains features of both systems and, in particular, is based on coupled ocean-atmosphere integrations as is the seasonal forecasting system.

The monthly forecasting system produces forecasts for the time range 10 to 30 days. At this time-range an important source of predictability is the the Madden-Julian Oscillation. The MJO has a significant impact on the Indian summer monsoon (Yasunari 1979). Clouds associated with the active phase of the monsoon propagate northward through the Indian ocean and Indian subcontinent at about 1 degree latitude per day (Murakami 1976). Yasunari (1979) associated these northward moving clouds to the MJO. It has a significant impact on the Australian monsoon (Hendon and Liebman 1990) and may play an active role in the onset and development of an El-Niño event (Kessler and McPhaden 1995). It also has an impact on tropical cyclogenesis over the eastern North Pacific (Maloney et al 2000) and over the Gulf of Mexico (Mo, 2000).

It can also affect the extratropics. Ferranti et al (1990) demonstrated that the MJO had a significant impact on Northern Hemisphere weather, including over Europe. They demonstrated, that there was a link between the MJO and PNA and North Atlantic Oscillation (NAO) teleconnection patterns. They provided evidence that an improved representation of the MJO in the ECMWF forecast model (achieved in that case by relaxing the tropical circulation towards analysis) could lead to a considerable increase of skill for the extratropics after 10 days of forecast. This result suggests that the MJO is an important source of predictability for the intraseasonal time range (more than 10 days and less than a season). Therefore it is very important for the monthly forecasting system to have skill in predicting the evolution of the MJO.

2 The ECMWF monthly forecasting system

The monthly forecasts at ECMWF are based on an ensemble of 51 coupled ocean-atmosphere integrations (one control and 50 perturbed forecasts). The length of the coupled integration is 32 days, and the frequency of the monthly forecasts is currently every 2 weeks. The atmospheric component is IFS with the same cycle as the ECMWF operational forecast. Currently, the atmospheric model is run at T_L159 resolution ($1.125^o \times 1.125^o$) with 40 levels in the vertical. This represents a resolution in between the ensemble prediction system (EPS) (T_L255L40) and seasonal forecasting (T_L95L40). The oceanic component is the same as for the current ECMWF seasonal forecasting system. It is HOPE (Wolff et al, 1997), from the Max Plank Institute. The atmosphere and ocean communicate with each other through a coupling interface, called OASIS (Terray et al, 1995), developed at CERFACS. The atmospheric fluxes of momentum, heat and fresh water are passed to the ocean every hour.

Atmospheric and land surface initial conditions are obtained from the ECMWF operational atmospheric analysis/reanalysis system. Oceanic initial conditions originate from the oceanic data assimilation system used to produce the initial conditions of the seasonal forecasting system 2. However, this oceanic data assimilation system lags about 12 days behind real-time. In order to 'predict' the ocean initial conditions, the ocean model is integrated from the last analysis, forced by analyzed wind stress, heat fluxes and P-E from the operational analysis. During this 'ocean forecast', the sea surface temperature is relaxed towards persisted SST, with a damping rate of 100 W/m^2/K. This method allows us to produce monthly forecasts in 'real-time' without having to wait for the ocean analysis to be ready.

The monthly forecasting system is run 51 times from slightly different initial conditions. One forecast, called the control, is run from the operational ocean and atmosphere ECMWF analyses. The 50 additional integrations, the perturbed members, are made from slightly different initial atmospheric and oceanic conditions, which are designed to represent the uncertainties inherent in the operational analyses. The 50 perturbations are produced using the singular vector method (Buizza and Palmer, 1995). These include perturbations in the extratropics and perturbations in some tropical areas by targeting tropical cyclones (Puri et al, 2001). In addition, in order to take into account the effect of uncertainties in the model formulation, the tendencies in the atmospheric physics are randomly perturbed during the model integrations. The current implementation is the same as that used in EPS. The oceanic initial conditions are perturbed in the same way as in seasonal forecasting system 2. Wind stress perturbations are applied during the data assimilation in order to produce five different ocean analyses, and SST perturbations are added to the ocean initial states.

After 10 days of coupled integrations, the model drift begins to be significant. The drift is removed from the model solution during the post-processing. In the present system, the climatology (back-statistics) is a 5-member ensemble of 32-day coupled integrations, starting on the same day and month as the real-time forecast for each of the past 12 years. This represents a total of 60 integrations and constitutes the 60-member ensemble of the back-statistics. The back statistics are created every 2 weeks, alternately with the real-time forecast. The ECMWF monthly forecasting system has been run routinely since 27 March 2002, and the present study is based on the verification of 30 cases.

3 The MJO in the monthly forecasting system

In order to evaluate the skill of the monthly forecasting system to predict the MJO, an EOF analysis of velocity potential anomalies (relative to the past 12-year climate) at 200 hPa has been performed on operational analyses and on each member of the monthly forecast. The velocity potential has been averaged between 5S and 5N along the whole equatorial band. For each member of the ensemble, all the 32-day forecasts of 200 hPa velocity potential anomalies (relative to the model climate) have been concatenated into a single file, before the EOF analysis was performed. The same process has been applied to the analysis, using ERA40 data to compute the climate. In both analysis and monthly forecast, the two dominant EOFs each represent about 36% of the total variance of 200 hPa velocity potential, and together, they represent more than 70% of the total variance. The

patterns are very similar in the analysis and in the monthly forecast (Figure1).

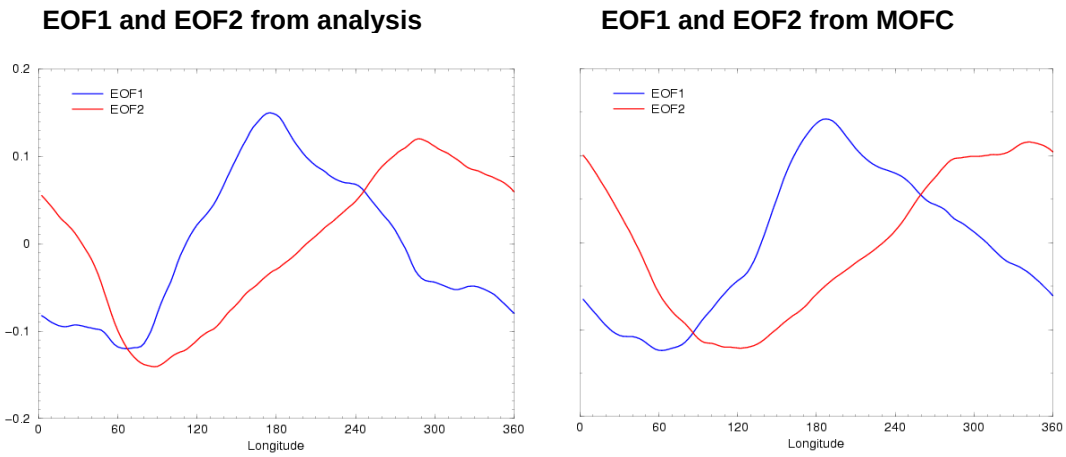

Figure 1: First 2 EOFs of velocity potential at 200 hPa computed from the analysis (left panel) and from the monthly forecasting system (right panel). For the monthly forecasting system, all lead times are included. The blue curve corresponds to the first EOF and the red curve corresponds to the second EOF. The x-axis represents the longitude.

The two dominant EOFs (EOF1 and EOF2) have a phase shift of about 90 degrees of longitude, which means that they capture the eastward propagation of velocity potential that is characteristic of an MJO event.

In order to evaluate the skill of the monthly forecasting system to predict the evolution of the MJO, for each longitudinal point (averaged from 5N to 5S) and for each time lag, the time series based on the 30 cases of the EOF-reconstructed 200 hPa velocity potential from the ensemble mean has been correlated with the time series computed using operational analysis and ERA40 (Figure2, middle panel). The linear correlation is above 0.6 up to 15 days over most longitudinal points, and remains high till about day 25. The linear correlations obtained are much higher than those obtained when persisting the initial condition (Fig.2, right panel). This suggests that the model has some skill in predicting the evolution of the MJO during at least the first 20 days of the forecast. The linear correlations are also higher than those obtained when using raw data of velocity potential instead of the EOF-reconstructed data. This is not surprising, since as mentioned above, the EOF-reconstructed data represents a filtered version of the velocity potential, and therefore is likely to be easier for the model to predict.

The skill of the monthly forecasting system to predict the Madden-Julian oscillation is confirmed when performing an anomaly correlation of the EOF-reconstructed velocity potential at 200 hPa averaged between 5S and 5N over the whole longitudinal band for each day of the forecast and for each case (Not shown). The scores of the monthly forecasting system are higher than with the control forecast, which is not surprising, since ensemble-means generally perform better than individual ensemble members. The score is also higher than when persisting the initial state. The RMS error of the ensemble-mean is lower than the RMS error obtained with persistence (Not shown). Interestingly, it is also lower than the RMS error obtained with climatology till around day 20. Therefore, the model displays useful skill in predicting the evolution of the MJO for about 20 days. This is in good agreement with the skill of statistical forecasts, such as the one by Wheeler and Weickmann (2001). This skill is likely to improve the scores of the monthly forecasting system in the extratropics.

Although the monthly forecasting system displays some skill in predicting the evolution of the MJO up to 20 days, it does not maintain the intensity of the MJO for more than a few days (Fig.3). The variance of the principal component (PC1) which is a measure of the intensity of the MJO is reduced by almost a factor 2 after only 10 days into a forecast. The dramatic reduction of variance is also present in PC2 (Not shown), although to a lesser extent.

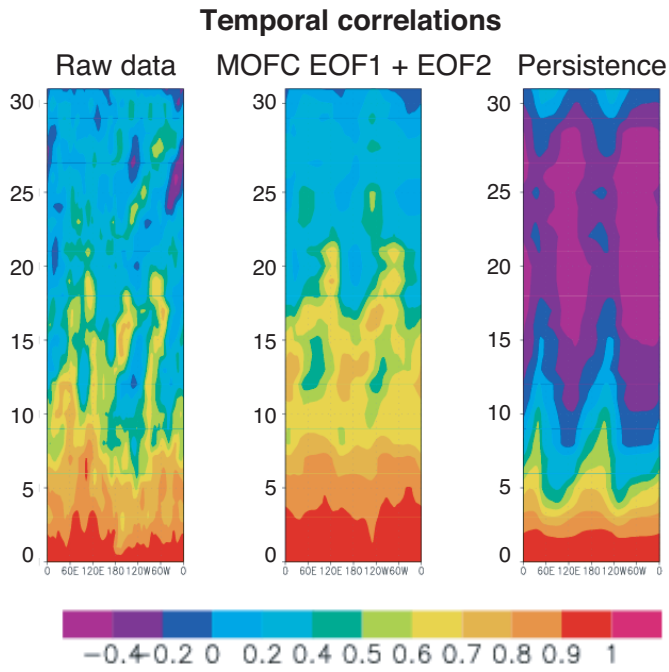

Figure 2: Hovmoller diagram of linear correlation between the time series of 200 hPa velocity potential anomaly predicted by the monthly forecasting system and the analysis (left panel). The middle panel shows the anomaly correlation obtained with the 200 hPa velocity potential anomaly after EOF reconstruction, instead of the raw data. The right panel shows the anomaly correlation obtained with persistence of the initial condition. The correlations have been computed from the 30 cases from March 2002 to May 2003.

All the 51 members of the monthly forecasting system have been projected into the PC1-PC2 phase-space. PC1 and PC2 are the two principal components associated with EOF1 and EOF2 computed from analysis and displayed in the left panel of Figure1. In the PC1-PC2 phase-space (see for instance Figure4), the distance from the origin represents the amplitude of the MJO and the positive x-axis (PC1 positive and PC2 equals to zero) corresponds to a velocity potential with the same shape as the EOF1 (blue curve) in Figure1 and therefore with a minimum at about 60E. Since the MJO is associated with *negative* values of the velocity potential, the positive x-axis corresponds roughly to an MJO at about 60E. In the same way, the positive y-axis corresponds to an MJO at about 90E. The negative x-axis corresponds to an MJO located at the dateline and the negative y-axis to an MJO at 60W. Therefore, the top right quadrant corresponds to the MJO over the Indian Ocean between approximatively 60E and 90E. The top left quadrant corresponds to the MJO over the central Pacific. The bottom left quadrant corresponds to an MJO further east between 180E and 60W. Finally the bottom right quadrant, corresponds to the MJO between 60W and 60E. So an MJO starting over the Indian Ocean and propagating all around the globe will be the arc of a circle starting in the top right quadrant in the PC1-PC2 phase space and moving anti-clockwise. The size of the domain corresponding to each quadrant varies since the two dominant EOFs (left panel in Figure1) are not exactly 90 degrees out of phase.

From the 30 cases that have been verified, it appears that the skill of the model to predict the MJO depends strongly on the initial position in the PC1-PC2 phase-space (Fig.4). In Figure 4, a cluster of bad cases at day 10 is present in the top right quadrant, which represent cases where the initial condition includes convection in the Indian Ocean. On the other hand, when the initial condition includes convection east of the maritime continent (large negative values of PC1 or large negative values of PC2), the model performs significantly better. Figure 4 suggests strongly that the monthly forecasting system has difficulties in propagating an MJO from the Indian Ocean to the Pacific. This is also true for verification at day 20, instead of day 10 (not shown). For day 20, most of the best cases have initial conditions clustered in regions of high negative PC1.

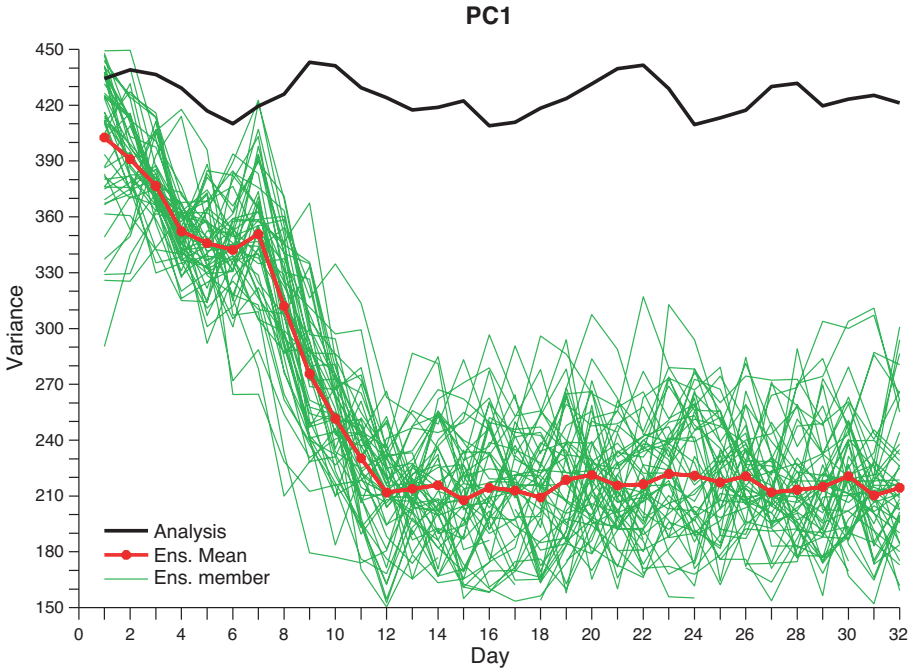

Figure 3: Time evolution of the amplitude of the principal component 1 (PC1). The black line corresponds to the analysis. Each green line represents the variance of one member of the ensemble averaged over the 30 cases. The solid red line represents the variance averaged over the 51 members of the ensemble. The variance has been computed over 30 cases from March 2002 to May 2003.

On the other hand, when the forecast starts with an MJO in the Pacific (see Figure 5 for instance), then the model seems to successfully predict its propagation. In Figure 5, the initial condition includes an MJO event near the dateline. The model successfully predicted its propagation during the first 20 days of the forecast. At day 20, the majority of ensemble members are in the same quadrant as the analysis, which, once again, is inside the cloud defined by all the monthly forecast ensemble members.

4 Conclusion

An experimental monthly forecasting system has been set up at ECMWF based on coupled 32-days ocean-atmosphere integrations. The skill of the monthly forecasting system to predict the evolution of the MJO has been evaluated through an EOF analysis of velocity potential at 200 hPa.

The monthly forecasting system does not have problems in producing eastward propagation of convection in the Tropics, but the model seems to have difficulty in propagating the convection from the Indian Ocean to the Pacific Ocean. This may be due to errors in the model mean state. The fact that the model physics did not maintain the intensity of the MJO suggests that part of the skill of the model to predict the propagation of the MJO was probably 'wasted' and did not contribute as much as expected to improve the skill of the monthly forecast system in the extratropics after 10 days.

The present paper has focused on the intraseasonal variability at 200 hPa. However, the MJO propagation is also present at lower levels of the troposphere, and can be diagnosed through OLR or low-level wind propagations. In general, GCMS get better intraseasonal propagation at 200 hPa than in the lower levels of the troposphere. Therefore, further plans include looking at combined EOFs of velocity potential at 200 hPa, OLR and winds at 850 hPa. This would give a more accurate and complete view on the skill of the ECMWF monthly forecasting

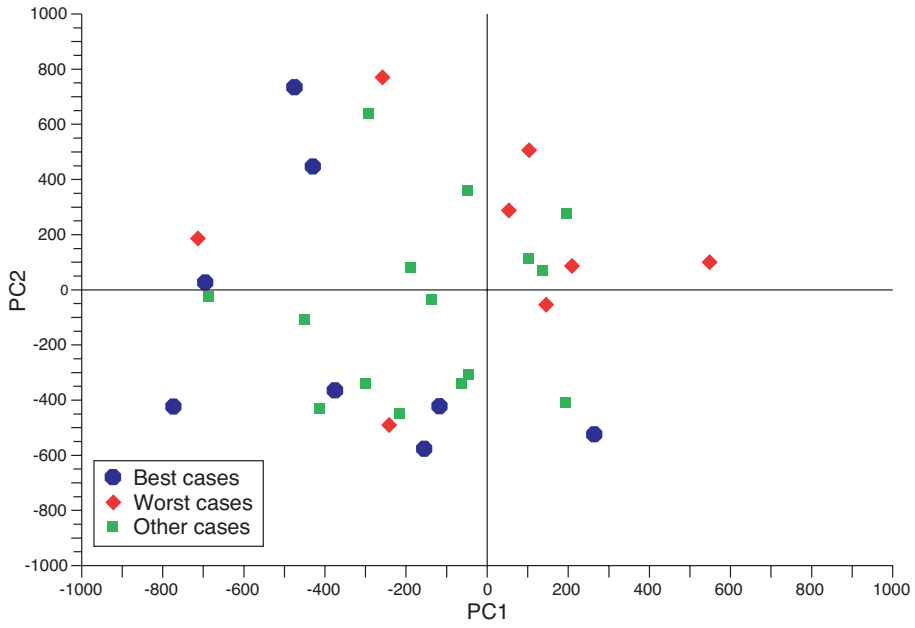

Figure 4: Initial positions of the 30 real-time monthly forecasts from March 2002 to May 2003 in the PC1-PC2 phase-space. The Blue circles represent the positions of the 8 best cases (25% of the cases) and the red diamonds represent the positions of the 8 worst cases at day 10. The skill of the forecast has been measured using the RMS error between the position of the analysis in the phase-space at day 10 and each individual member of the ensemble.

system to predict the MJO propagation. In addition, more cases studies will be available in order to study the skill of the model to predict the genesis of an MJO event.

REFERENCES

Buizza, R. and T.N. Palmer, 1995: The singular-vector structure of the atmospheric global circulation. *J. Atmos. Sci.*, **52**, 1434-1456.

Ferranti, L., T.N. Palmer, F. Molteni, and E. Klinker, 1990: Tropical-extratropical interaction associated with the 30-60 day oscillation and its impact on medium and extended range prediction. *J. Atmos. Sci.*, **47**, 2177-2199.

Hendon, H.H., and B. Liebmann, 1990: A composite study of onset of Australian summer monsoon. *J. Atmos. Sci.*, **47**, 2909-2923.

Kessler, K.S. and M.J. McPhaden, 1995: Oceanic equatorial Kelvin waves and the 1991-1993 El-Nino. *J. Climate*, **8**, 1757-1774.

Maloney, E.D. and D.L. Hartmann, 2000: Modulation of eastern North Pacific hurricanes by the Madden-Julian oscillation. *J. Climate*, **13**, 1451-1460.

Mo, K.C., 2000: The association between intraseasonal oscillations and tropical storms in the Atlantic basin, *Mon. Wea. Rev.*, **128**, 4097-4107.

Murakami, T., 1976: Cloudiness fluctuations during the summer monsoon. *J. Meteor. Soc. Japan*, **54**, 175-181.

Puri, K., Barkmeijer, J., Palmer, T.N., 2001: Tropical singular vectors computed with linearized diabatic physics. *Quart. J. Roy. Meteor. Soc.*, **127**, 709-731.

Terray, L., E. Sevault, E. Guilyardi and O. Thual, 1995: The OASIS coupler user guide version 2.0, *CERFACS*,

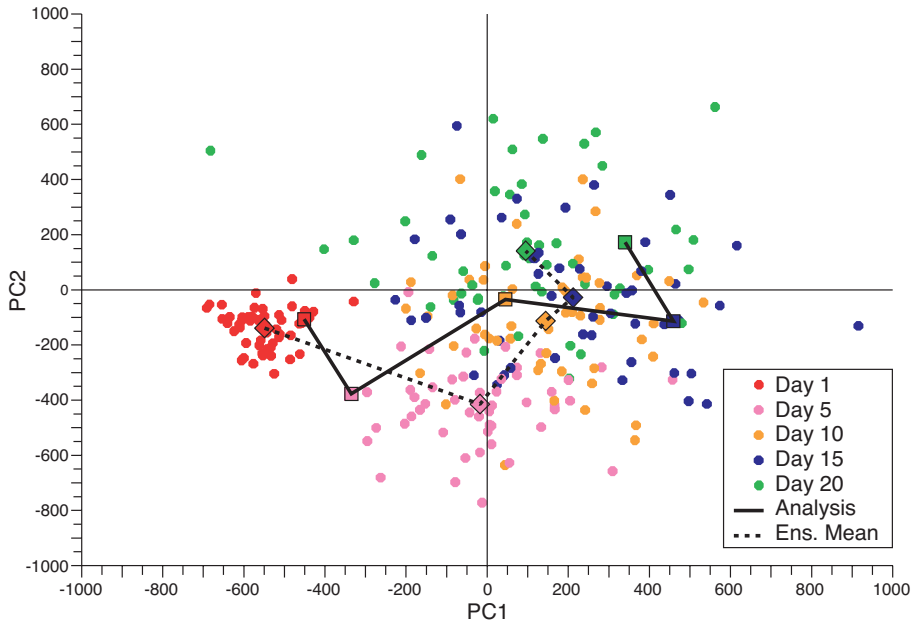

Figure 5: Monthly forecast starting on 4 June 2003 in the PC1-PC2 phase space. Each circle represents one member of the monthly forecast after 1 day (red), 5 days (magenta), 10 days (orange), 15 days (blue) and 20 days (green). The big squares and the solid line represent the operational analysis. The dotted line represents the position averaged over all the members of the ensemble. The top right quadrant corresponds to an MJO activity in the Indian Ocean between 60E to 90E. The top left quadrant corresponds to an MJO activity between 90E and 180E. The bottom left quadrant corresponsd to an MJO east of the dateline but west of 60W. Finally, the bottom right quadrant corresponds to an MJO activity between 60W and 60E.

technical report, TR/CMGC/95-46.

Wheeler, M., and K.M. Weickmann, 2001: Real-Time Monitoring and Prediction of Modes of Coherent Synoptic to Intraseasonal Tropical Variability. *Mon. Wea. Rev.*, **129**, 2677-2694.

Wolff, J.O., E. Maier-Raimer and S. Legutke, 1997: The Hamburg Ocean Primitive Equation Model. *Deutches klimarechenzentrum, Hamburg, Technical Report*, **13**, 98 pp.

Yasunari, T., 1979: Cloudiness fluctuations associated with the Northern Hemisphere summer monsoon. *Meteor. Soc. of Japan*, **58**, 225-229.